Alphaherpesvirus axon-to-cell spread involves limited virion transmission

Matthew P. Taylor[a], Oren Kobiler[b,1], and Lynn W. Enquist[a,1]

[a]Department of Molecular Biology, Princeton University, Princeton, NJ 08544; and [b]Department of Clinical Microbiology and Immunology, Sackler School of Medicine, Tel Aviv University, Tel Aviv, 69978 Israel

Edited by Bernard Roizman, University of Chicago, Chicago, IL, and approved September 5, 2012 (received for review July 27, 2012)

The spread of viral infection within a host can be restricted by bottlenecks that limit the size and diversity of the viral population. An essential process for alphaherpesvirus infection is spread from axons of peripheral nervous system neurons to cells in peripheral epithelia (anterograde-directed spread, ADS). ADS is necessary for the formation of vesicular lesions characteristic of reactivated herpesvirus infections; however, the number of virions transmitted is unknown. We have developed two methods to quantitate ADS events using a compartmentalized neuronal culture system. The first method uses HSV-1 and pseudorabies virus recombinants that express one of three different fluorescent proteins. The fluorescence profiles of cells infected with the virus mixtures are used to quantify the number of expressed viral genomes. Strikingly, although epithelial or neuronal cells express 3–10 viral genomes after infection by free virions, epithelial cells infected by HSV-1 or pseudorabies virus following ADS express fewer than two viral genomes. The second method uses live-cell fluorescence microscopy to track individual capsids involved in ADS. We observed that most ADS events involve a single capsid infecting a target epithelial cell. Together, these complementary analyses reveal that ADS events are restricted to small numbers of viral particles, most often a single virion, resulting in a single viral genome initiating infection.

cell–cell spread | live-cell imaging

Viral infections begin when infectious virus particles (virions) attach to and enter susceptible cells. After this initial event, infection can spread either locally or across long distances via hematogenous, lymphatic, or neural routes. In either case, spread from cell to cell often involves direct transmission of infectious particles with no or limited release of infectious particles into the extracellular milieu (1). Cell-to-cell spread of some infections, such as HIV, involves transfer of many viral particles (2), whereas other infections, such those caused by poliovirus, involve transfer of small numbers of particles (3). Virions of members of the alphaherpesvirinae, including the human pathogens HSV-1 and HSV-2, varicella zoster virus, and the animal pathogen pseudorabies virus (PRV) infect epithelial surfaces and transmit efficiently to innervating axons of the peripheral nervous system (PNS) (4). Viral particle transport within neurons and spread to epithelial cells is essential for the propagation of infection, yet the number of virions transmitted between cells during these spread events is unknown.

After primary infection of natural hosts, alphaherpesvirus genomes are usually maintained in a quiescent state in sensory and autonomic ganglia until extrinsic or intrinsic factors stimulate productive viral replication in neuronal cell bodies (5). A subset of progeny virions produced in neuronal cell bodies is sorted into axons and transported to sites of egress, usually at the epithelial surface where the primary infection initiated (6). After egress from axons, susceptible cells in the mucosal epithelia or skin are infected, often resulting in characteristic vesicular herpetic lesions (4). Spread of infection from cell bodies of sensory neurons and their axons to peripheral epithelial cells is termed anterograde-directed spread (ADS). Here, we developed two methods to quantify the number of virions that spread from axons and replicate in epithelial cells using a well-characterized in vitro model for ADS of alphaherpesviruses (7, 8). The first method uses a mixed infection of isogenic recombinant viruses, each expressing a different fluorophore to calculate the average number of genomes expressed in infected cells. The second method uses live-cell imaging of fluorescently tagged virions to observe and track virion egress from PNS axons and subsequent entry into susceptible epithelial cells. Using these complementary methods we demonstrate that ADS involves a remarkably small number of virions, with the majority of cells becoming infected by a single virion.

Results

Construction and Characterization of Isogenic HSV-1 and PRV Recombinants That Express Fluorescent Proteins. To determine the number of viral genomes that initiate infection in epithelial cells after ADS, we expanded a previously published method to determine the number of expressed genomes. The distribution of fluorescent protein expression in a population of infected cells is fit to a Poisson-distribution model to calculate the average number of actively replicating viral genomes (9). It was important for these studies that the replication of these viruses be as similar as possible yet express different fluorophores. To this end, we isolated isogenic HSV-1 and PRV viral strains that express mCereluean, EYFP, or mCherry tagged with a nuclear localization signal (NLS) as described in *Materials and Methods*. All recombinants replicated with equal efficiency in epithelial cells (Fig. 1 *A* and *E*) in a single growth curve on Vero or PK15 cells. The capacity for ADS was tested in compartmentalized neuronal cultures described in the following section. All recombinant viruses of HSV and PRV demonstrated an equivalent capacity for anterograde spread and replication in chambered neuronal cultures (Fig. 1 *C*, *D*, *G*, and *H*).

Using the three new PRV recombinants, we confirmed that even at high multiplicities of infection (MOI), only a limited number of viral genomes are expressed and replicated in porcine kidney epithelial (PK15) cells (9). At the highest MOI used (100 pfus per cell), less than eight PRV genomes were expressed per cell on average, in concordance with previous results (9) (Fig. 1*F* and Table 1). Similar results were obtained with the three HSV-1 recombinants in that fewer than 10 viral genomes were expressed in Vero cells, even at a MOI of 100 (Fig. 1*B* and Table 1). Importantly, the limit on genome expression was similar in neurons as it was in epithelial cell lines: approximately eight HSV-1 or PRV genomes were expressed in PNS neurons (Rat superior cervical ganglia, SCG) at the highest infectious dose (Table 1). SCG's are autonomic ganglia that are readily dissociated and cultured as a homogenous population of neurons. SCG neuron cultures have been extensively used to study the replication and

Author contributions: M.P.T., O.K., and L.W.E. designed research; M.P.T. and O.K. performed research; M.P.T. and O.K. contributed new reagents/analytic tools; M.P.T., O.K., and L.W.E. analyzed data; and M.P.T., O.K., and L.W.E. wrote the paper.

The authors declare no conflict of interest.

This article is a PNAS Direct Submission.

[1]To whom correspondence may be addressed. E-mail: okobiler@post.tau.ac.il or Lenquist@princeton.edu.

This article contains supporting information online at www.pnas.org/lookup/suppl/doi:10.1073/pnas.1212926109/-/DCSupplemental.

Downloaded by guest on January 23, 2021

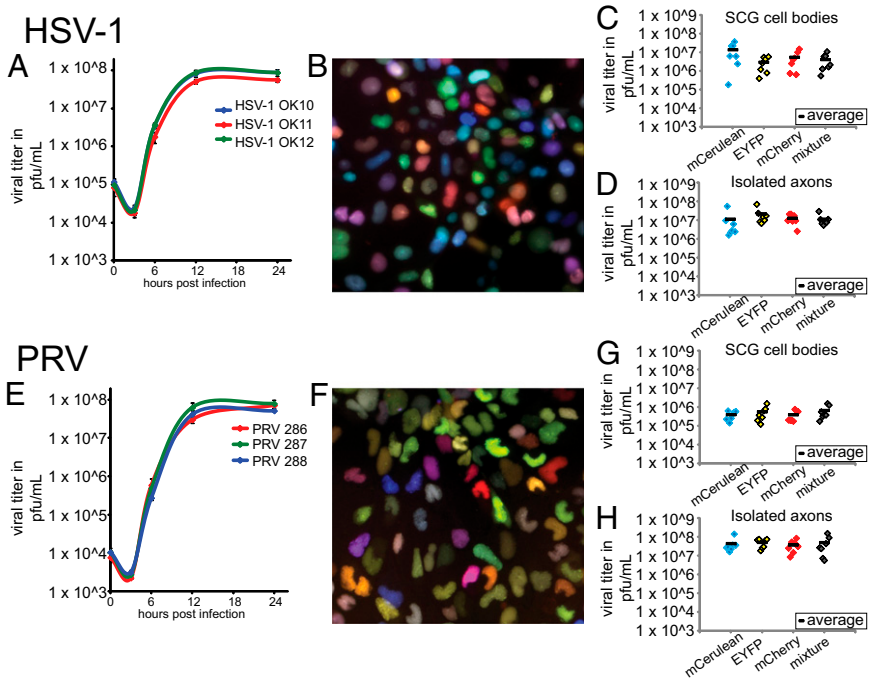

Fig. 1. Testing isogenic HSV and PRV XFP-NLS viruses. Three isogenic viruses for either HSV-1 strain 17 (*A–D*) or PRV (*E–H*) were tested for replication and anterograde directed spread. (*A*) Vero cells or (*E*) PK15 cells were infected with individual HSV or PRV strains at a MOI of 10 and harvested at 0, 6, 12, and 24 h postinfection. Viral titers were determined by limiting dilution on their respective cell lines. (*B* and *F*) Representative images taken with a 20× magnification objective of a MOI 100 infection with a mixture of the three fluorophore expressing strains used to calculate the maximum average genome expression value (Table 1). (*C*, *D*, *G*, and *H*) Individual viruses and a mixture of all three viruses were used to infect the neuronal cell bodies. (*C* and *G*) Viral titers from neuronal cell bodies or (*D* and *H*) isolated axon extensions in compartmentalized neuronal culture harvested 48 and 24 h postinfection, respectively.

spread of alphaherpesviruses. We conclude that the limitation on the number of expressed viral genomes is essentially the same for HSV-1 as it is for PRV. Furthermore, the limitation for both viruses is not dependent on cell type. We also conclude that the expressed fluorescent proteins do not introduce a bias in the replication, expression, or transmission for any one of the recombinants.

Quantification of Genome Diversity in Epithelial Cells Following ADS. To visualize and quantify the transmission of HSV-1 and PRV recombinant viruses from axons to epithelial cells, we used a compartmentalized neuronal culture system previously developed to measure ADS (7). Briefly, a three-compartment Teflon ring attached to a dish by silicon grease enables the culture of SCG neuron cell bodies in one compartment, termed the soma or S compartment, and grooves in the dish direct axonal extensions to migrate underneath two silicon grease barriers and enrich in a neurite or N compartment (Fig. 2*A*). After SCG axons extend into the N compartment (~14–21 d), epithelial cells are added as a confluent monolayer, simulating the distal axon environment near peripheral mucosa. This system facilitates the physical separation of primary infection of neuronal cell bodies from subsequent ADS events in the epithelial cell compartment.

Table 1. Average viral genome expression in epithelial cells and neurons

Cell lines and neurons	Infectious dose	HSV-1	PRV
Epithelial cell lines	MOI 5	3.52 ± 0.77	3.10 ± 0.29
	10	3.89 ± 0.95	3.90 ± 0.53
	50	8.74 ± 1.40	5.86 ± 0.62
	100	9.76 ± 1.14	7.98 ± 1.01
Neurons	1×10^5 pfu	4.90 ± 0.96	6.84 ± 2.43
	5×10^5	4.81 ± 1.74	7.88 ± 1.98
	1×10^6	7.50 ± 1.94	8.39 ± 1.63
ADS infected cells		1.40 ± 0.09	1.63 ± 0.07

Equivalent mixtures of HSV-1 or PRV recombinant viruses were used to infect Vero, PK15, or SCG cells at the indicated infectious dose. Titers of these recombinants were determined on PK15 cells for PRV and Vero cells for HSV-1. The average expressed viral genome number was calculated as described in *Materials and Methods*. Each value is shown with SD and represents 3,600 cells per condition from two experiments for both Vero and PK15 cells from images taken at 6–8 h postinfection and over 1,000 SCG cells per condition taken at 8–10 h postinfection. For axon-to-cell ADS events, a minimum of 600 cells across four chambers (two chambers per experiment) were tracked for each virus.

The cell bodies of compartmentalized SCG neurons were infected with an equal mixture of the three isogenic HSV-1 or PRV recombinant viruses (Fig. 2*B*). After 24 or 48 h, epithelial cells cultured in the N compartment were imaged for fluorescent protein expression. After HSV-1 infection of SCG cell bodies, ADS in the epithelial cell compartment was remarkably focal, with many pure-color patches of infected epithelial cells (Fig. 2 *C* and *D* and Movie S1). After PRV infection of SCG cell bodies, ADS was more widespread, and pure-color sectors of infected epithelial cells were less distinct (Fig. 2*E* and Movie S1). The monochromatic sectors most likely result from a single epithelial cell expressing a single viral genome (one color) infected by ADS. Moreover, the extensive infection of the epithelial cell layer observed during PRV most likely reflects more ADS egress events.

We tested these possibilities by time-lapse microscopy of ADS infection events in the susceptible detector cell monolayer of the N compartment, starting at 6 h postinfection of the neuronal cell body compartment for PRV or 16 h postinfection for HSV (Movie S1). The initial ADS events were defined as the first cells in the detector epithelial cell layer that began to express fluorescent proteins. Individual cells expressing a detectable fluorescence profile (Fig. 2 *D* and *E*) were marked, tracked by time-lapse

Downloaded by guest on January 23, 2021

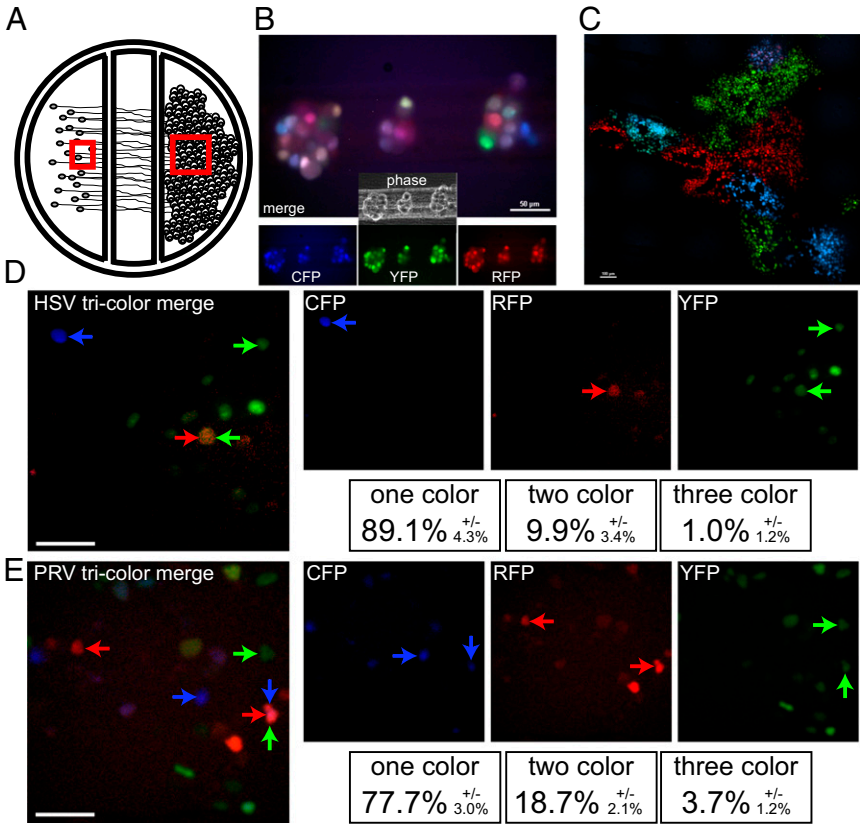

Fig. 2. Three-color infection of compartmentalized neuronal cultures. (*A*) Schematic representation of compartmentalized neuronal culture system. Dissociated SCG cell bodies are plated in the far left soma (S) compartment and neurite extensions penetrate underneath two sequential barriers and extend into the far right neurite (N) compartment. Epithelial cells (Veros or PK15s for HSV and PRV, respectively) are plated onto the isolated neurites 1 d before neuron cell body infection. Red squares indicate the area imaged in *B* (*Left* box) and *C* (*Right* box). (*B*) SCG cells bodies in the S compartment were imaged 8 h after infection with a mixture of HSV-1 strain 17 that expresses mCereulean, EYFP, or mCherry. A merged image of all three fluorescent channels is presented with individual channels and phase-contrast image is inset below. (Scale bar, 50 μm.) (*C*) Vero detector cells plated on isolated neurites in the N compartment were imaged 48 h after neuronal cell body infection for fluorescence expression. A merged image of the three fluorescent channels is presented. (Scale bar, 100 μm.) (*D*) A representative image taken from time lapse imaging of the Vero detector cells demonstrating the spatially isolated initial infection of individual cells from isolated axons. Single-color, two-color, and three-color cells are marked as indicated. (Scale bar, 50 μm.) (*E*) A representative image taken from time lapse imaging of the PK15 detector cells labeled as described for *D* (Scale bar, 50 μm.)

microscopy, and quantified for fluorescent protein expression. The color spectrum of almost all HSV-1–infected cells and about 90% of PRV-infected cells remained constant over time. As suggested from data in Fig. 2, the majority of cells infected through ADS expressed only one fluorophore. For PRV infections, more than 77% of ADS events were single color. For HSV infections, almost 90% of ADS events were single color (Fig. 2*D*). From these distributions, we calculated that, on average, 1.4 HSV genomes and 1.6 PRV genomes were expressed in epithelial cells after ADS (Table 1). Mixed infection of SCG neurons with PRV or HSV recombinant viruses resulted in 80% triply infected cells capable of producing a mixed population of virions for long-distance axonal transport. Therefore, ADS events for both HSV-1 and PRV genomes represent a previously unrecognized bottleneck that substantially reduces diversity of the viral population spreading from axons into epithelial cells.

Visualization of Single ADS Events Using Epithelial Cell "Island" Microcolonies. To visualize the transfer of virus particles from axons to cells, we imaged isolated axons in close opposition to individual PK15 cells. To do this, we first plated SCG neurons in the cell body compartment, allowed axon extension to occur, and then plated PK15 cells at low density in the axon compartment, where they formed small microcolony "islands" adjacent to or underneath isolated axonal extensions. These PK15 microcolonies facilitated visualization of capsid transmission from closely apposed axons to single PK15 cells. SCG cell bodies were then infected with a PRV recombinant that expresses two fluorescent markers: a farnesylated YFP (YFP-CAAX) to mark membranes of infected cells and a VP26-mRFP fusion to visualize capsids. YFP-CAAX expression is driven by the HCMV immediate-early promoter, and thus, labels the plasma and internal membranes by 1–2 h after infection. VP26-mRFP expression is driven by the late VP26 promoter that is active only after viral DNA replication initiates. Imaging conditions were optimized to reduce photodamage by reducing the required excitation light intensity and performing short burst, time-lapse imaging over many hours.

Because the image acquisition rate is one every 5 min, fluorescent VP26-mRFP puncta produced in the isolated SCG cell bodies and sorted into axons move hundreds of microns between frames, consistent with previous estimates of axonal transport (Fig. 3 *B–D* and Movie S2) (10, 11). When VP26-mRFP puncta leave axons and enter epithelial cells, they associate at or near the nucleus. These infected cells then quickly express farnesylated YFP on membranes followed by intense expression and accumulation of the late protein, VP26-mRFP, in the nucleus (Fig. 3*D*).

Productive Individual Axon-to-Cell Capsid Transmission Events Involves a Small Number of Viral Particles. We identified productive ADS egress events after imaging random fields of PK15 island microcolonies for 16 h. Each movie was then manually examined for individual infected PK15 cells (the point of initial YFP expression followed by VP26-mRFP expression) and run backward until the initial infection event was observed. Productive egress/entry events were scored after appearance of VP26-mRFP puncta in the phase image of the cell. Capsid puncta were counted if they were detected in association with the nucleus for a minimum of three sequential frames (15 min). Images of representative PK15 cells with visible VP26-mRFP puncta are shown (Fig. 3 *E* and *F* and Movies S3 and S4). We imaged a total of 157 infected cells across three independent experiments, and counted the capsids associated with each cell before YFP expression. (Fig. 3*G*). Surprisingly, almost half of the infections clearly initiated with a single, detectable, VP26-mRFP puncta before the expression of YFP. A smaller population initiated with two-to-four capsid puncta and less than 8% of infected cells initiated with more than 5 and as many as 15 capsids. Infection-initiating events of more than five capsids often were preceded

Downloaded by guest on January 23, 2021

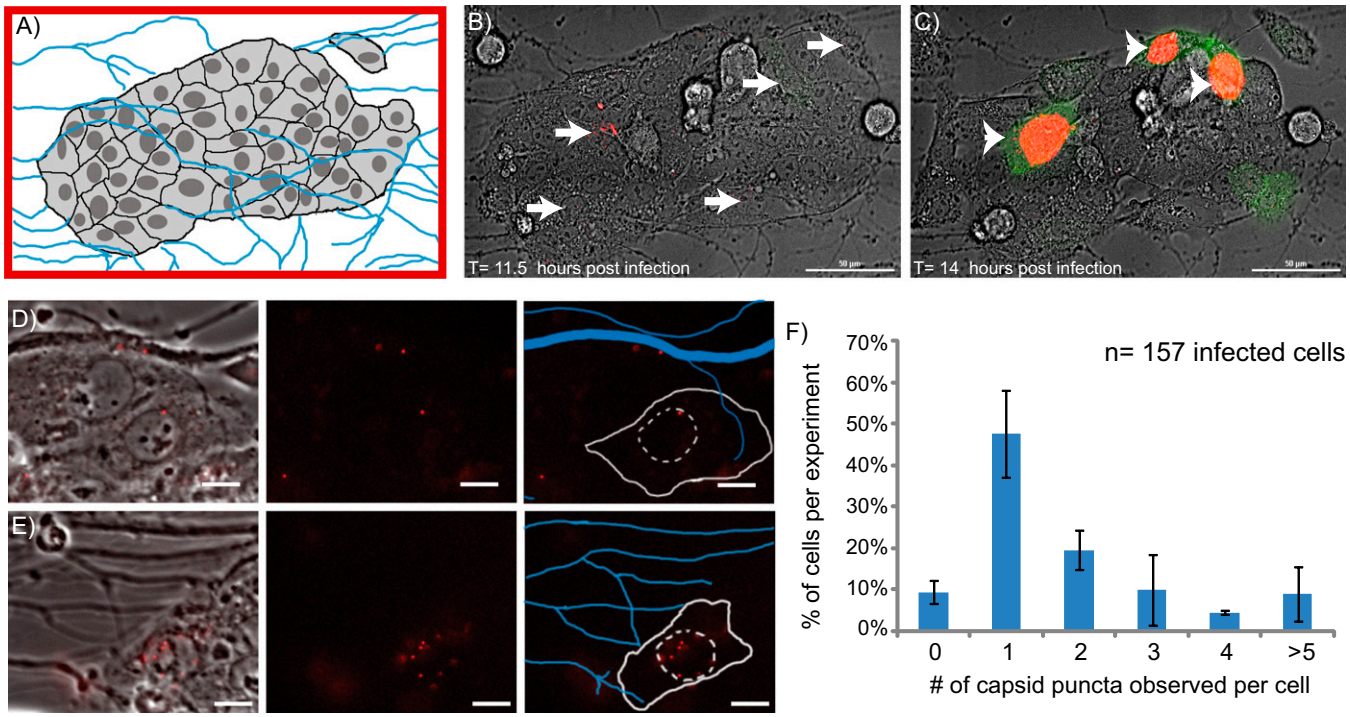

Fig. 3. Live-cell imaging of PK15 islands during axon-to-cell infection. (*A*) Schematic representation of the "island" of multiple PK15 cells that seeded in close association with isolated neurite extensions in the far right compartment of compartmentalized neuronal cultures. Axon tracks are highlighted in blue. Approximate cell boundaries marked in black and nuclei annotated as dark gray circles. (*B* and *C*) Sequential images from the time-lapse recording are presented. (Scale bar, 100 μm.) (*B*) At 11.5 h postinfection, mRFP puncta become associated with the nuclei of the PK15 cells. (*C*) At 14 h postinfection, many of these cells (large white arrowheads) begin to accumulate detectable amounts of farnesylated YFP, indicative of successful infection by the virus. (*D* and *E*) Two representative infected cells after virion entry and before expression of viral proteins. A merged mRFP fluorescence and phase image is presented (*Left*), mRFP fluorescence (*Center*), and mRFP fluorescence with an overlay of the approximate locations of axons and the infected cell (*Right*). Approximate cell periphery is outlined in a solid white line; the nucleus is outlined with a dashed white line, axons are blue. (Scale bars, 10 μm.) (*D*) A single cell with a single mRFP-puncta associated with the nucleus of the cell. (*E*) A cell infected with a large number of virions, greater than five. (*F*) The number of virions per infected cell was counted across three experiments for a total of 157 infected cells. The number of cells containing 0, 1, 2, 3, 4, or >5 capsids is expressed as a percent of the total infected cells per experiment and averaged across all three experiments. Error bars represent SD between experiments.

by an accumulation of VP26-mRFP puncta in axons close to the cell that subsequently became infected. These multicapsid events may represent a unique egress process distinct from the majority of initiating events involving only one virion. Less than 10% of the total infected cells observed have no detectable capsid present during the course of imaging. Despite these limitations, our data indicate that in the majority of ADS events, a limited number of virions are transmitted from axons to susceptible cells.

Discussion

We previously identified a limitation in the number of PRV genomes able to be expressed and replicated in a single infected cell (9). Here, we corroborate this observation and show that it occurs also for HSV-1 expression and can be detected in primary neuronal cells as well as epithelial cell lines. We therefore suggest that this bottleneck is a general phenomenon of alphaherpesvirus infection. We used an in vitro chambered neuronal culture system to model spread of alphaherpesvirus infection from axons to epithelial cells (ADS). We found, using two complementary methods, that the vast majority of ADS events involved one or two single egressing infectious particles. Initially, we determined the number of viral genomes expressed following ADS by tricolor infections using mixtures of isogenic HSV and PRV recombinant viruses. To confirm and extend this result, we visualized the number of particles that initiate single ADS events through live-cell imaging of fluorescently tagged PRV virions. These complementary analyses indicate that the majority of ADS events are restricted to one or two virions, yet are exceptionally efficient in delivering one or two genomes to initiate viral replication. This previously unrecognized bottleneck in transmission of HSV or PRV virions from axons to susceptible cells is more strict than the previously described limitation on the number of viral genomes that are expressed and replicated in the nucleus. This ADS bottleneck further limits the overall diversity of the progeny herpesvirus population during propagation of viral infections within a host.

The efficiency of ADS events is remarkable (one or two viral particles are sufficient to initiate viral replication in an epithelial cell), particularly because the particle-to-pfu ratio of stocks of PRV virions grown in cultured cells is reported to be in the range of 20–50 (12–14). It is possible that fully functional viral particles are selectively sorted and transported into axons as opposed to the particles produced during standard stock production. It also is likely that egressing virions are not exposed to the culture milieu or other inactivating events that typify standard infection conditions. Further studies will be needed to distinguish between these possibilities.

The bottleneck in transmission of HSV or PRV from axons to susceptible cells presumably occurs between the point of virion egress from the infected axon and delivery of viral genomes into the nucleus of the newly infected cell. Multiple virions are transported to distal axon sites, as can be seen from our time-lapse movies (Movies S2, S3, and S4) as well as previously published data (11), suggesting that many virions could be transmitted at any one time. Despite a single virion infecting susceptible cells, the remaining virions that undergo transport may be able to initiate

Downloaded by guest on January 23, 2021

infection, although this possibility has not been tested. The restriction is not because of superinfection exclusion in the epithelial cells, which requires expression of glycoprotein gD (15, 16), although it is possible that further virion entry is blocked by the activation of intrinsic cellular defense mechanisms (17, 18). It is likely that the interface between the axon and cellular membranes plays a major role in regulating the number of virions that spread to susceptible cells. Previous reports noted the presence of axonal varicosities at or near putative axonal egress sites (19), as well as an accumulation of capsids within varicosities and axon termini (20). Although the vast majority of ADS events observed in our system involve single capsids, a small number (8%) involved more than five capsids, and these events may well be occurring at varicosities or synapses; sites where capsids accumulate before egress. The viral and cellular proteins that associate and coordinate particle egress from axons remain poorly characterized and are the subject of continued investigation.

Transmission bottlenecks are well known for a number of plant and mammalian viruses. Studies of plant RNA viruses generally report small effective population sizes during transmission, whereas studies with one plant DNA virus reported a large population of virions during spread in single plant (21–23). The transmission of HIV between T cells involves transmission of a large number of virions across a virological synapse (2, 24). The same concept has been suggested for HSV-1 transmission in T cells (25). Studies of the retrograde transneuronal transmission of poliovirus identified a bottleneck during axonal transport (3, 26). Kuss et al. marked poliovirus genomes with nucleic acid "bar codes" to follow spread of infection of virus populations into the PNS and CNS (27). In these studies, population diversity diminished as the length of axon increased. Poliovirus mutants that could not produce the normal diversity of wild-type virus populations were less able to infect the brain and cause disease. Although it is assumed that PRV and HSV-1 do not produce the prodigious diversity generated by RNA viruses during replication, our study identified a distinct restriction of axon-epithelial cell spread of infection at or near the point of egress. This restriction point may not be unique to the alphaherpesviruses. Many viruses that infect the nervous system, including members of the rhabdoviridae and paramyxoviridae, spread between synaptically connected cells, taking advantage of neuronal architecture to transmit infection long distances within an infected host (28). Testing these viruses in our experimental systems may establish if these infections are also restricted at the point of axon-to-cell spread.

The extent of alphaherpesvirus diversity during replication in vitro and in vivo and the effect of transmission bottlenecks have not been studied extensively. Previously, it was demonstrated that the protein composition of individual virus particles produced in cultured cells varies considerably (10, 29, 30). Recently, using high-throughput DNA sequencing, it has become clear that there is substantial diversity in herpesvirus genomes (31). The importance of this diversity for the fitness of herpesvirus infection is not well known. There is some evidence that transneuronal spread of attenuated strains of PRV involves a limited number of genomes, which would limit diversity (32). Our work demonstrates that a small number of virus particles are involved in ADS, limiting whatever diversity exists during transmission. This bottleneck in spread from neurons to epithelial cells would limit opportunities for complementation and recombination among viral genomes at peripheral sites. Mutant genomes or defective interfering genomes (33, 34) that require coinfection for replication would be selected against after axonal spread to epithelial cells, effectively increasing the overall fitness of the spreading viral population. A major effect of population bottlenecks is that they directly affect the adaptability of viral infection to immune responses and drug treatments by altering fitness. Expanding our current studies to determine the effect of this population bottleneck on in vivo propagation and spread of alphaherpesviruses will increase our understanding of this group of persistent and pervasive pathogens.

Materials and Methods

Viruses and Cells. The porcine kidney epithelial cell line PK15 was used to propagate and titer all PRV viral strains. The African green monkey kidney epithelial cell line Vero was used to propagate and titer all HSV-1 viral strains. All cell lines were maintained in DMEM supplemented with 10% (vol/vol) FBS and 1% (vol/vol) Penicillin/Streptomycin. To construct the viruses used in the three-color coinfection model, we designed three plasmids containing a CMV modified immediate-early promoter driving the expression of a fluorescent protein fused to a tandem triplet repeat of a NLS, RSRADPKKKRKVDPKKKRKVDPKKKRKVGSR, terminated with a SV40 polyA sequence. NLS targeted fluorophores (XFP-NLS) were chosen for their superior capacity to separate the fluorescence profile of closely apposed cells, compared with previously used diffuse fluorophores. The fluorophore expression cassettes containing either, mCeruelean, EYFP, or mCherry and ~500 bp of HSV-1 strain17 UL37, UL38 region [a locus shown previously to tolerate insertion of the selection cassette necessary for BAC generation without significant reduction in viral titers (35)] homologous sequence flanking the 5′ and 3′ ends of the cassette were synthesized (GenScript). Linearized plasmids were cotransfected into Vero cells with HSV-1 strain17 DNA. Colored plaques were selected and purified on Vero cells. Similarly, the same plasmids described above were used for cotransfection with nucleocapsid DNA of PRV151 a wild-type PRV Becker derivative expressing EGFP (36). The original EGFP cassette at the gG locus of this strain was replaced with the XFP-NLS cassettes by homologous recombination between the CMV promoter and SV40polyA sequences. Colored plaques were selected and purified on PK15 cells. To generate the virus used for live particle imaging, PRV 151 was first recombined with PRV 180 (VP26-mRFP) (29) to produce the intermediate virus PRV 426, which expresses the VP26-mRFP fusion protein and diffusible GFP. Nucleocapsid DNA of PRV 426 was then cotransfected with a YFP-CAAX domain expression plasmid (a kind gift of the T. Meyer Laboratory, Stanford University, Stanford, CA). Plaques expressing VP26-mRFP and plasma membrane bound YFP were visually selected and purified on PK15 cells to generate PRV 427.

Compartmentalized Neuronal Culturing. Primary neuronal cultures of SCG neurons were maintained in neuronal media, which consists of Neurobasal Media (Invitrogen) supplemented with 1% (vol/vol) penicillin/streptomycin-glutamine (Invitrogen), B27 Supplement (Invitrogen), and 50 ng/mL Neuronal Growth Factor 2.5S (NGF) (Invitrogen). Before neuron plating, cell-culture surfaces were coated with poly-ornithine (Sigma-Aldrich) at 500 μg/mL in borate buffer (pH 8.2) followed by murine laminin (Invitrogen) at 10 μg/mL in calcium and magnesium-free HBSS. Compartmentalized neuronal cultures were prepared as described in ref. 7. Briefly, plastic tissue culture dishes were treated as described above, parallel grooves were etched into the surface, and a 1% (wt/vol) methylcellulose/1× DMEM solution was spotted on the grooves. CAMP320 Teflon isolator rings (Tyler Research) were coated with autoclaved vacuum grease on one side and gently applied to the treated culture surface such that the parallel grooves extended across the three compartments. Approximately 8,000 dissociated SCG neurons were plated into one side compartment (S compartment). Cultures were maintained until axon extensions had robustly penetrated and grown into the far side compartment (N compartment).

SCG neuron cultures were not infected until 17–24 d of culturing to allow for full neuronal maturation. One day before infection, ~5×10^5 Vero or PK15 cells (for HSV and PRV infections, respectively) in 1% (vol/vol) FBS supplemented neuronal media were plated on top of the isolated axons in the N compartment (Fig. 2*A*). The cells amplified anterograde spreading virions in the N compartment, enhancing detection of spread events. Before the application of viral inoculum to the S compartment, 1% (wt/vol) methylcellulose supplemented neuronal media was placed within the middle compartment. Dissociated or compartmentalized SCG neuronal cultures were infected with ~1×10^6 pfu of virus in 100 μL of conditioned neuronal media. Inoculum was replaced after 1 h with the original volume of conditioned growth media.

Imaging for Expressed Genome Quantitation. We obtained images of cells infected with equal amounts of three viruses at different MOIs (100, 50, 10, and 5) and estimated the number of viral genomes expressed in each infected cell as previously described (9). In brief, all epifluorescence imaging was performed on a Nikon Ti-Eclipse inverted microscope equipped with separate fast-switching excitation and emission filter wheels (Prior Scientific) using a Plan Fluor 20×Ph objective (Nikon). For each experimental condition at least 3,600 cells were analyzed for the presence of the three colors (two

Downloaded by guest on January 23, 2021

experiments, three replicate wells in each, at each well three random image areas were collected and more than 200 cells per area were analyzed). The mathematical equation for estimating the most likely average number of genomes expressed in each cell (λ) according to the number of one- (r_1), two- (r_2), or three-color (r_3) cells of the number of cells analyzed (n) was previously developed (9):

$$\lambda = -3\ln\left(1 - \frac{r_1 + 2r_2 + 3r_3}{3n}\right)$$

Here we have used this equation for estimating the number of genomes expressed following infection with high titers of either HSV-1 or PRV either of epithelial cell lines or of SCG neurons, as we suspect these infection processes are similar. Similarly, we used the same equation for estimating the number of genomes expressed following axonal egress events, because these events are random, independent of each other, and are relatively rare, all characteristics of Poisson variable. In agreement with our assumption is that the distribution of individual viral particles events is similar to Poisson distribution (not including the multicapsid events).

Viral Particle Imaging. Compartmentalized neuronal cultures were constructed as described above on optical plastic dishes (Ibidi). One day before infection, $\sim 1 \times 10^4$ PK15 cells were sparsely seeded onto isolated axons in the far compartment. Methylcellulose [1% (wt/vol) final concentration]-supplemented media was applied to the cells immediately before infection. Viral inoculum was applied to the S compartment and the PK15s were visualized by fluorescent imaging beginning approximately 5 h postinfection. Overnight movies were acquired either every 5 or 20 min with phase, YFP and RFP fluoresence using a 60× Plan Fluor Ph3 objective (Nikon) at 37 °C in a 5% (vol/vol) CO_2 enriched atmosphere using a stage top incubator system (Quorum Scientific). Multiple image fields we collected and large image areas were observed using the image tiling module of NIS-Elements.

Virion Quantitation. Virion number was quantified by tracking cells that expressed detectable YFP at any point during the overnight imaging course. RFP puncta that became associated with the cell for a minimum of three consecutive frames were counted until the detectable expression of YFP was observed. Cells that expressed YFP but lacked any associated capsid were marked zero.

ACKNOWLEDGMENTS. L.W.E. is supported by the National Institutes of Health Grants R37 NS033506-16 and R01 NS060699-03 and M.P.T. is supported by American Cancer Society Postdoctoral Research Fellowship PF-10-057-01-MPC.

1. Mothes W, Sherer NM, Jin J, Zhong P (2010) Virus cell-to-cell transmission. *J Virol* 84: 8360–8368.
2. Del Portillo A, et al. (2011) Multiploid inheritance of HIV-1 during cell-to-cell infection. *J Virol* 85:7169–7176.
3. Pfeiffer JK (2010) Innate host barriers to viral trafficking and population diversity: lessons learned from poliovirus. *Adv Virus Res* 77:85–118.
4. Smith GA (2012) Herpesvirus transport to the nervous system and back again. *Annu Rev Microbiol* 66:153–176.
5. Knipe DM, Cliffe A (2008) Chromatin control of herpes simplex virus lytic and latent infection. *Nat Rev Microbiol* 6:211–221.
6. Kratchmarov R, Taylor MP, Enquist LW (2012) Making the case: Married versus separate models of alphaherpes virus anterograde transport in axons. *Rev Med Virol* 16: 1–12.
7. Ch'ng TH, Enquist LW (2005) Neuron-to-cell spread of pseudorabies virus in a compartmented neuronal culture system. *J Virol* 79:10875–10889.
8. Ch'ng TH, Enquist LW (2006) An in vitro system to study trans-neuronal spread of pseudorabies virus infection. *Vet Microbiol* 113:193–197.
9. Kobiler O, Lipman Y, Therkelsen K, Daubechies I, Enquist LW (2010) Herpesviruses carrying a Brainbow cassette reveal replication and expression of limited numbers of incoming genomes. *Nat Commun* 1:146.
10. Smith GA, Gross SP, Enquist LW (2001) Herpesviruses use bidirectional fast-axonal transport to spread in sensory neurons. *Proc Natl Acad Sci USA* 98:3466–3470.
11. Antinone SE, Zaichick SV, Smith GA (2010) Resolving the assembly state of herpes simplex virus during axon transport by live-cell imaging. *J Virol* 84(24):13019–13030.
12. Flint SJ; American Society for Microbiology (2009) *Principles of Virology* (ASM, Washington, DC), 3rd Ed pp 2 v. xxii, 569, 419 p.
13. Harland J, Brown SM (1998) HSV growth, preparation, and assay. *Methods Mol Med* 10:1–8.
14. Frenkel N, et al. (1975) Anatomy of herpes simplex virus DNA. III. Characterization of defective DNA molecules and biological properties of virus populations containing them. *J Virol* 16:153–167.
15. Campadelli-Fiume G, et al. (1990) Glycoprotein D of herpes simplex virus encodes a domain which precludes penetration of cells expressing the glycoprotein by superinfecting herpes simplex virus. *J Virol* 64:6070–6079.
16. Petrovskis EA, Meyer AL, Post LE (1988) Reduced yield of infectious pseudorabies virus and herpes simplex virus from cell lines producing viral glycoprotein gp50. *J Virol* 62: 2196–2199.
17. Leoni V, Gianni T, Salvioli S, Campadelli-Fiume G (2012) Herpes simplex virus glycoproteins gH/gL and gB bind Toll-like receptor 2, and soluble gH/gL is sufficient to activate NF-κB. *J Virol* 86:6555–6562.
18. Rasmussen SB, et al. (2007) Type I interferon production during herpes simplex virus infection is controlled by cell-type-specific viral recognition through Toll-like receptor 9, the mitochondrial antiviral signaling protein pathway, and novel recognition systems. *J Virol* 81:13315–13324.
19. De Regge N, et al. (2006) Alpha-herpesvirus glycoprotein D interaction with sensory neurons triggers formation of varicosities that serve as virus exit sites. *J Cell Biol* 174: 267–275.
20. Saksena MM, et al. (2006) Herpes simplex virus type 1 accumulation, envelopment, and exit in growth cones and varicosities in mid-distal regions of axons. *J Virol* 80: 3592–3606.
21. Li H, Roossinck MJ (2004) Genetic bottlenecks reduce population variation in an experimental RNA virus population. *J Virol* 78:10582–10587.
22. Miyashita S, Kishino H (2010) Estimation of the size of genetic bottlenecks in cell-to-cell movement of soil-borne wheat mosaic virus and the possible role of the bottlenecks in speeding up selection of variations in trans-acting genes or elements. *J Virol* 84:1828–1837.
23. Roossinck MJ (2011) Changes in population dynamics in mutualistic versus pathogenic viruses. *Viruses* 3:12–19.
24. Hübner W, et al. (2009) Quantitative 3D video microscopy of HIV transfer across T cell virological synapses. *Science* 323:1743–1747.
25. Aubert M, Yoon M, Sloan DD, Spear PG, Jerome KR (2009) The virological synapse facilitates herpes simplex virus entry into T cells. *J Virol* 83:6171–6183.
26. Pfeiffer JK, Kirkegaard K (2006) Bottleneck-mediated quasispecies restriction during spread of an RNA virus from inoculation site to brain. *Proc Natl Acad Sci USA* 103: 5520–5525.
27. Kuss SK, Etheredge CA, Pfeiffer JK (2008) Multiple host barriers restrict poliovirus trafficking in mice. *PLoS Pathog* 4:e1000082.
28. Salinas S, Schiavo G, Kremer EJ (2010) A hitchhiker's guide to the nervous system: The complex journey of viruses and toxins. *Nat Rev Microbiol* 8:645–655.
29. del Rio T, Ch'ng TH, Flood EA, Gross SP, Enquist LW (2005) Heterogeneity of a fluorescent tegument component in single pseudorabies virus virions and enveloped axonal assemblies. *J Virol* 79:3903–3919.
30. Antinone SE, Smith GA (2006) Two modes of herpesvirus trafficking in neurons: Membrane acquisition directs motion. *J Virol* 80:11235–11240.
31. Renzette N, Bhattacharjee B, Jensen JD, Gibson L, Kowalik TF (2011) Extensive genome-wide variability of human cytomegalovirus in congenitally infected infants. *PLoS Pathog* 7:e1001344.
32. Card JP, et al. (2011) Microdissection of neural networks by conditional reporter expression from a Brainbow herpesvirus. *Proc Natl Acad Sci USA* 108:3377–3382.
33. Ben-Porat T, Demarchi JM, Kaplan AS (1974) Characterization of defective interfering viral particles present in a population of pseudorabies virions. *Virology* 61:29–37.
34. Denniston KJ, Madden MJ, Enquist LW, Vande Woude G (1981) Characterization of coliphage lambda hybrids carrying DNA fragments from Herpes simplex virus type 1 defective interfering particles. *Gene* 15:365–378.
35. Gierasch WW, et al. (2006) Construction and characterization of bacterial artificial chromosomes containing HSV-1 strains 17 and KOS. *J Virol Methods* 135:197–206.
36. Smith BN, et al. (2000) Pseudorabies virus expressing enhanced green fluorescent protein: A tool for in vitro electrophysiological analysis of transsynaptically labeled neurons in identified central nervous system circuits. *Proc Natl Acad Sci USA* 97: 9264–9269.

Downloaded by guest on January 23, 2021